

Photoionization of atoms with half-filled shells

M. Ya. Amus'ya, V. K. Dolmatov, and V. K. Ivanov

A. F. Ioffe Physicotechnical Institute, Academy of Sciences of the USSR, Leningrad

(Submitted 4 February 1983)

Zh. Eksp. Teor. Fiz. **85**, 115–123 (July 1983).

The method of random phases with exchange is generalized to take into account many-electron correlations in atoms with half-filled shells. The effect of correlations on photoionization cross sections and angular distributions of photoelectrons from chromium, manganese, and technetium atoms in the region of the $3p$ - and $4p$ -thresholds is investigated. It is shown that this region is dominated by a large peak of autoionization origin. The outer-shell level energies are determined for the manganese atom with allowance for many-electron correlations. Results of these calculations are in good agreement with experiment.

PACS numbers: 32.80.Fb, 32.80.Dz, 31.20.Tz

1. INTRODUCTION

The use of the mathematical formalism of the theory of the many-body problem and of the methods based upon it, e.g., the random phase approximation with exchange¹ (RPAE), has resulted in a satisfactory description of the photoionization process in the case of a large number of outer and intermediate shells of a series of atoms. The RPAE corrections for electron-electron correlations have turned out to be so significant that they have led to not only qualitative but also quantitative differences between the behavior of the photoionization cross section and the results obtained by different one-electron methods.¹ These data have formed the basis for the conclusion that photoabsorption in the outer and intermediate atomic shells is collective in character, and this is of fundamental importance for the theory of many-electron atoms.

However, the RPAE method is restricted in its application to atoms having closed shells. Direct application of the method and, for that matter, of the entire mathematical formalism of the theory of the many-body problem, to atoms with unfilled shells is difficult^{2,3} because the ground state of these atoms is degenerate.

In the present paper, we report a systematic generalization of the RPAE method to atoms with half-filled shells. For the single-particle basis, we take the spin-polarized Hartree-Fock approximation.⁴ This enables us to use the many-body formalism and, on this basis, additionally examine over twenty additional atoms in the periodic table.

The physical content of the spin-polarized approximation can be summarized as follows. In the ground state, Hund's rule demands that all the electron spins in the half-filled atomic shell point in the same direction, for example, upward (\uparrow). We shall refer to them as the up-electrons in contrast to electrons pointing downward (\downarrow), which will be referred to as down-electrons. The states of up- and down-electrons in a filled shell are now found to be different because they have different interactions with the up-electrons in the half-filled shell (with or without exchange). This leads to the splitting of the filled subshell into two different up- and down-levels. It is thus clear that the states of the electrons now depend on the quantum numbers n , l , and μ (μ is

the spin projection) and remain degenerate only in the projections of the orbital angular momentum m_l .

The equations for the one-electron wave functions and the energies of electrons in the spin-polarized variant of the Hartree-Fock approximation differ from the usual equations in that they take into account the exchange interaction only between electrons with the same values of μ . This means, in particular, that the total energy of the atom is lower than that obtained in the usual Hartree-Fock approach.

The level splitting that we are considering is much greater than the spin-orbit splitting. Moreover, it occurs even for the s -shells of atoms. For example, in the Mn atom with the half-filled $3d^5$ shell, the splitting of the $3s^2$ and the $3p^6$ shells is ~ 11 and ~ 13 eV, respectively,⁵ whereas the spin-orbit splitting of the $3p^6$ shell is ~ 1.4 eV.⁶ It follows that the spin-orbit interaction is small enough to be neglected in the first approximation. Since the Coulomb interaction cannot alter the component of the spin of the electrons, it will not result in a mixing of the up- and down-levels. The latter can therefore be regarded as filled, which enables us to apply the mathematical formalism of the theory of the many-body problem.

As an example, consider the electron structure of the ground state of the Mn atom in this approximation:

$$1s^{\uparrow}1s^{\downarrow}2s^{\uparrow}2s^{\downarrow}2p^{\uparrow}2p^{\downarrow}3s^{\uparrow}3s^{\downarrow}3p^{\uparrow}3p^{\downarrow}3d^{\uparrow}4s^{\uparrow}4s^{\downarrow}.$$

The application of the generalized RPAE method, which is based on the spin-polarized Hartree-Fock approximation, will now be illustrated by calculations of the photoionization cross sections of Cr, Mn, and Tc atoms and the angular distributions of photoelectrons in the region of the $3p\downarrow$ (for Cr and Mn) and $4p\downarrow$ (for Tc) ionization thresholds. It will be shown that, in this region, the cross section has a giant autoionization peak with a width of $\gamma \gtrsim 1$ eV, which is much greater than the usual width of ~ 0.01 – 0.1 eV. The calculations performed for Cr and Mn atoms are in good agreement with existing experimental data.^{7–10}

The splitting of atomic shells into the up- and down-sublevels should, of course, lead to the appearance of additional thresholds in different atomic reactions. In the last

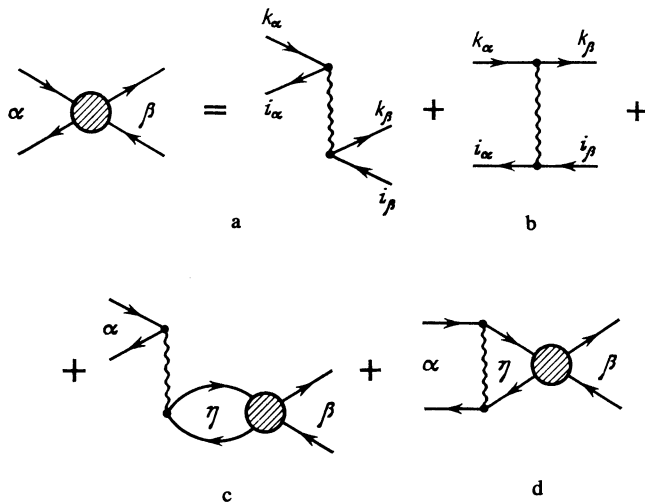


FIG. 1. Equation for the determination of the effective interaction Γ .

section, we report calculations of these thresholds for the outer subshells of Mn with allowance for the rearrangement of the atom that produces a large level shift but has a smaller effect on the level splitting.

2. RPAE EQUATIONS FOR THE EFFECTIVE INTERACTION AND THE PHOTOIONIZATION AMPLITUDE

The basic equation in the RPAE method is the equation for the matrix elements of the effective interaction Γ .¹ It is shown in Fig. 1 with the aid of the Feynman diagrams for atoms with closed shells. Lines with arrows pointing to the right (left) correspond to a particle (hole) in the atom, and a wavy line and a shaded block correspond to the Coulomb V and the effective Γ interactions, respectively; the subscripts α, β, η label states of the particle-hole pairs.

In the method developed in the present paper, the atom is looked upon as a system consisting of nonequivalent up- and down-electrons. The particle-hole up- and down-pairs can be arranged in different ways in the initial, intermediate, and final states, and the resulting equations are different from one another. Neglecting spin-dependent interactions, and recalling that the contribution of the exchange diagrams b and d must be excluded when α and β are states with different spin components, we obtain a set of four coupled equations that are conveniently written in the matrix form

$$\begin{pmatrix} \Gamma_{\alpha\beta}^{\uparrow\uparrow} & \Gamma_{\alpha\beta}^{\uparrow\downarrow} \\ \Gamma_{\alpha\beta}^{\downarrow\uparrow} & \Gamma_{\alpha\beta}^{\downarrow\downarrow} \end{pmatrix} = \begin{pmatrix} U_{\alpha\beta}^{\uparrow\uparrow} & V_{\alpha\beta}^{\uparrow\downarrow} \\ V_{\alpha\beta}^{\downarrow\uparrow} & U_{\alpha\beta}^{\downarrow\downarrow} \end{pmatrix} + \begin{pmatrix} U_{\alpha\eta}^{\uparrow\uparrow} & V_{\alpha\eta}^{\uparrow\downarrow} \\ V_{\alpha\eta}^{\downarrow\uparrow} & U_{\alpha\eta}^{\downarrow\downarrow} \end{pmatrix} \begin{pmatrix} \chi_{\eta}^{\uparrow} & 0 \\ 0 & \chi_{\eta}^{\downarrow} \end{pmatrix} \begin{pmatrix} \Gamma_{\eta\beta}^{\uparrow\uparrow} & \Gamma_{\eta\beta}^{\uparrow\downarrow} \\ \Gamma_{\eta\beta}^{\downarrow\uparrow} & \Gamma_{\eta\beta}^{\downarrow\downarrow} \end{pmatrix} \quad (2.1)$$

where arrows indicate the type (up or down) of particle-hole pairs for whose states the matrix elements are being evaluated ($U_{\alpha\beta}$ include the Coulomb matrix elements $V_{\alpha\beta}$ and the exchange-interaction matrix elements $V_{\alpha\beta}^{\text{exch}}$); χ_{η} is the operator defined by

$$\hat{U}_{\alpha\eta}\hat{\chi}_{\eta}\hat{\Gamma}_{\eta\beta} = \sum_{\eta} \left(\frac{\hat{U}_{\alpha\eta}\hat{\Gamma}_{\eta\beta}}{E_{\alpha}^p - E_{\alpha}^h - E_{\eta}^p + E_{\eta}^h + i\delta} - \frac{\hat{U}_{\alpha\eta}\hat{\Gamma}_{\eta\beta}}{E_{\alpha}^p - E_{\alpha}^h + E_{\eta}^p - E_{\eta}^h - i\delta} \right), \quad (2.2)$$

where the operator symbol emphasizes that this expression is a matrix in the indices \uparrow and \downarrow .

The sum is evaluated over all the possible states of the particle-hole pairs in the intermediate state η ; E^p and E^h are the particle and hole energies in the respective particle-hole pairs, and the term $i\delta$ ($\delta \rightarrow +0$) indicates the rule for bypassing the singularity during integration over the continuous spectrum.

The above form of the matrix elements is equivalent, for example, to the following:

$$\Gamma_{\alpha\beta} = \langle i_{\alpha} k_{\beta} | \hat{\Gamma} | k_{\alpha} i_{\beta} \rangle, \quad (2.3)$$

$$U_{\alpha\beta} = \langle i_{\alpha} k_{\beta} | V | k_{\alpha} i_{\beta} \rangle - \langle i_{\alpha} k_{\beta} | V | i_{\beta} k_{\alpha} \rangle,$$

where $k(i)$ is the state of the particle (hole) in the corresponding particle-hole pair (Fig. 1).

The equation for the photoionization amplitude of an atom with allowance for electron correlations can be expressed directly in terms of the matrix elements of the effective interaction.¹ In our approach, the photoionization amplitudes corresponding to the removal of up- or down-electrons from the atom turn out to be different. Proceeding by analogy with the determination of the matrix elements of the effective interaction, we obtain

$$(D_{\alpha}^{\uparrow}, D_{\alpha}^{\downarrow}) = (d_{\alpha}^{\uparrow}, d_{\alpha}^{\downarrow}) + (d_{\eta}^{\uparrow}\chi_{\eta}^{\uparrow}, d_{\eta}^{\downarrow}\chi_{\eta}^{\downarrow}) \begin{pmatrix} \Gamma_{\eta\alpha}^{\uparrow\uparrow} & \Gamma_{\eta\alpha}^{\uparrow\downarrow} \\ \Gamma_{\eta\alpha}^{\downarrow\uparrow} & \Gamma_{\eta\alpha}^{\downarrow\downarrow} \end{pmatrix}, \quad (2.4)$$

where D_{α} and d_{α} are, respectively, the amplitudes for the excitation of the atom with the formation of the electron-hole state α when (1) allowance is made for correlations and (2) the Hartree-Fock approximation is employed. The operator χ_{η} is defined by a condition analogous to (2.2) in which, in accordance with energy conservation, ($E_{\alpha}^p - E_{\alpha}^h = E_{\beta}^p - E_{\beta}^h = \omega$) (ω is the energy of the incident photon and we put $\hbar = 1$).

The photoionization cross section of the atom is related to the amplitude D_{α} in the usual way (see, for example, Ref. 1).

Equations (2.1) and (2.4) are the basic equations in our method. When the states of the up- and down-electrons are equivalent, Eqs. (2.1) and (2.4) become identical with the usual equations of the RPAE method.¹ In this sense, our equations constitute a generalization of the RPAE method to include atoms with half-filled shells.

3. GIANT AUTOIONIZATION IN Cr, Mn AND Tc ATOMS

We have used the above generalization of RPAE to consider the photoionization of atoms with a half-filled nd^5 shell: Cr and Mn with $n = 3$, and Tc with $n = 4$. We shall confine our attention here to incident-photon energies in the neighborhood of the ionization threshold for the shell pre-

ceding the half-filled shell: $3p^3 \downarrow$ for Cr and Mn, and $4p^3 \downarrow$ for Tc.

In the one-electron approximation, the photoionization cross section in this region is a continuous function of the photon energy, and is largely determined by the $nd \uparrow \rightarrow \epsilon f \uparrow$ transition to the continuous spectrum (ϵ is the energy of the photoelectron). When intra-shell and inter-shell correlations are taken into account, this results in only a small change in the cross section, with the exception of the $nd \uparrow \rightarrow \epsilon f \uparrow$ interaction and the discrete $np \downarrow \rightarrow nd \downarrow$ transition. The latter has a large oscillator strength and its inclusion produces a large, broad autoionization peak. The photoionization process along two main channels, namely:

$$np^3 \downarrow nd^5 \uparrow + \omega \rightarrow np^3 \downarrow nd^4 \uparrow \epsilon f \uparrow, \quad (3.1)$$

$$np^3 \downarrow nd^5 \uparrow + \omega \rightarrow np^2 \downarrow nd^5 \uparrow nd \downarrow \rightarrow np^3 \downarrow nd^4 \uparrow \epsilon f \uparrow. \quad (3.2)$$

Direct calculation of the photoionization cross section from (2.1) and (2.4) with $\omega = \omega_s$ (ω_s is the excitation energy of a discrete level) is not possible because the denominator is then equal to zero. We must therefore separate the divergent element in the amplitude for the phototransition to the continuous spectrum α . In the neighborhood of the resonance this amplitude can be written in the form

$$\mathcal{D}_\alpha^\dagger(\omega) = D_\alpha^\dagger(\omega) + \frac{D_s^\dagger(\omega) \Gamma_{s\alpha}^{\dagger\dagger}(\omega)}{\omega - \omega_s - \Gamma_{s\alpha}^{\dagger\dagger}(\omega)}, \quad (3.3)$$

where D_α^\dagger is the amplitude for the direct transition to the continuous spectrum $nd^4 \uparrow \epsilon f \uparrow$, given by (2.4) with the discrete $np \downarrow \rightarrow nd \downarrow$, transition excluded; the second term describes the process proceeding in accordance with (3.2). In (3.3), the quantity D_s^\dagger is the amplitude for the excitation of the $np^2 \downarrow nd^5 \uparrow nd \downarrow$ level, which is also determined from (2.4) by analogy with D_α^\dagger ; $\Gamma_{s\alpha}^{\dagger\dagger}$ is the matrix element of the interaction between the discrete transition and the continuous spectrum, and $\Gamma_{ss}^{\dagger\dagger}$ is the matrix element of the effective interaction of the discrete level with itself through the excitation of the states α . The matrix elements $\Gamma_{s\alpha}^{\dagger\dagger}$ and $\Gamma_{ss}^{\dagger\dagger}$ are solutions of (2.1), in which $\eta \neq s$.

The interaction between the discrete excitation of $np^2 \downarrow nd^5 \uparrow nd \downarrow$ and the continuum leads to a shift of the position of the resonance level relative to ω_s and to the appearance of the level width γ . The new position of the resonance, $\tilde{\omega}_s$, is given by

$$\tilde{\omega}_s - \omega_s - \text{Re} \Gamma_{s\alpha}^{\dagger\dagger}(\tilde{\omega}_s) = 0. \quad (3.4)$$

Expanding $\text{Re} \Gamma_{s\alpha}^{\dagger\dagger}(\omega)$ in powers of $(\omega - \tilde{\omega}_s)$ and retaining first-order terms only, we obtain the amplitude (3.3) in the form

$$\mathcal{D}_\alpha^\dagger(\omega) = D_\alpha^\dagger(\omega) + \frac{D_s^\dagger(\omega) \Gamma_{s\alpha}^{\dagger\dagger}(\omega)}{(\omega - \tilde{\omega}_s) [1 - (\partial \text{Re} \Gamma_{s\alpha}^{\dagger\dagger} / \partial \omega)_{\omega = \tilde{\omega}_s}] + i\gamma/2}. \quad (3.5)$$

Multiplying the numerator and the denominator by the renormalizing factor

$$F = [1 - (\partial \text{Re} \Gamma_{s\alpha}^{\dagger\dagger} / \partial \omega)_{\omega = \tilde{\omega}_s}]^{-1},$$

we obtain

$$\mathcal{D}_\alpha^\dagger(\omega) = D_\alpha^\dagger(\omega) + \frac{D_s^\dagger \tilde{\Gamma}_{s\alpha}^{\dagger\dagger}}{\omega - \tilde{\omega}_s + i\tilde{\gamma}/2}, \quad (3.6)$$

where

$$\tilde{\gamma} = F\gamma = -2F \text{Im} \Gamma_{s\alpha}^{\dagger\dagger}, \quad \tilde{D}_s^\dagger = F^{1/2} D_s^\dagger, \quad \tilde{\Gamma}_{s\alpha}^{\dagger\dagger} = F^{1/2} \Gamma_{s\alpha}^{\dagger\dagger}.$$

If we neglect the dependence of the matrix elements on ω near the resonance, and evaluate them at $\omega = \tilde{\omega}_s$, we find that (3.6) becomes identical with the usual Fano formula for the photoionization cross section near a resonance¹¹:

$$\sigma = \sigma_a \frac{(\xi + q)^2}{\xi^2 + 1} + \sigma_b, \quad \xi = \frac{2(\omega - \tilde{\omega}_s)}{\gamma}, \quad (3.7)$$

where σ_a , σ_b , q , and γ are the parameters of the line profile, which are defined in terms of the amplitudes introduced above.

However, owing to the large width of the resonance in atoms with unfilled shells, the profile parameters cannot, strictly speaking, be regarded as constants. The dependence of $\text{Re} \Gamma_{s\alpha}^{\dagger\dagger}$ on ω has the greatest influence on the behavior of the resonance cross section, and its inclusion has an immediate effect on the width of the profile, leading to its renormalization. The renormalized factor F will also modify the parameters σ_a and σ_b , but has no effect on q because $q = -\text{Re} D_s^\dagger / \text{Im} D_\alpha^\dagger$. In our calculations, we were able to neglect the dependence of D_s^\dagger and D_α^\dagger on ω and, hence, the dependence of $\Gamma_{s\alpha}^{\dagger\dagger}(\omega)$ and $\gamma(\omega)$ on ω , since these quantities are defined by

$$\Gamma_{s\alpha}^{\dagger\dagger} = -\frac{\text{Im} D_s^\dagger}{\pi |D_\alpha^\dagger|^2} D_\alpha^\dagger, \quad \gamma = 2\pi |\Gamma_{s\alpha}^{\dagger\dagger}|^2. \quad (3.8)$$

Table I shows the values of the profile parameters ω_s , γ , q , σ_a and σ_b calculated within the RPAE framework. The width of the profile was calculated with ($\tilde{\gamma}$) and without (γ) renormalization. In addition to the Hartree-Fock transition energy ω_s , we also give the value of $\tilde{\omega}_s$, calculated from (3.4). The experimental parameter values were obtained from

TABLE I. Energy of discrete transitions to a half-filled shell and parameters of the autoionization resonance.

Atom	Transition Energy			ν , eV			q		σ_a , Mb	σ_b , Mb
	ω_s	$\tilde{\omega}_s$	exp	ν	$\tilde{\nu}$	exp	calc	exp		
Cr	46.8	44.9	43.7	1.3	0.78	0.75	3.4	3.1	7.9	0.3
Mn	52.8	50.4	49.8	2.0	1.40	1.30	2.5	2.3	7.6	0.3
Tc	42.4	41.7	—	5.5	2.10	—	2.0	—	12.0	1.2

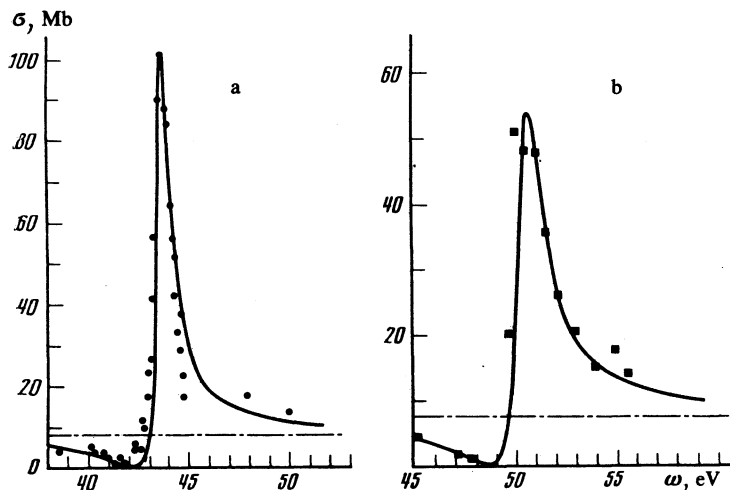


FIG. 2. Photoionization cross sections for Cr (a) and Mn (b) near the resonance transition to a half-filled shell: dot-dash line—without including the $3p \downarrow \rightarrow 3d \downarrow$ transition, solid lines—with allowance for the discrete $3p \downarrow \rightarrow 3d \downarrow$ transition, \blacksquare and \bullet —experimental data from Refs. 9 and 10, respectively.

Refs. 9 and 10 as a result of an analysis of the photoemission spectra of Cr and Mn. There are no experimental data for Tc.

It is clear from Table I that renormalization has an important effect on the width of the profile and leads to good agreement with experiment. To elucidate the physical meaning of the coefficient F , let us write down the expression for $-\partial \text{Re} \Gamma_{ss}^{-1} / \partial \omega$ in the lowest perturbation-theory order in the interaction:

$$-\frac{\partial \text{Re} \Gamma_{ss}^{-1}}{\partial \omega} \Big|_{\omega=\tilde{\omega}_s} = \sum_{\eta} \frac{|V_{\eta s}|^2}{(\tilde{\omega}_s - \omega_{\eta})^2}, \quad (3.9)$$

where the sum is evaluated over both discrete and continuous electron-hole states η coupled to the excitation s . The ratio $V_{\eta s} / (\tilde{\omega}_s - \omega_{\eta})$ is the (η, s) mixing amplitude, so that F is the fraction of the pure state s in the composite state that appears as a result of the interaction of the excitation s with the excitation η . We draw attention to the fact that the width

of the peak is greater for Tc than for Cr. This is connected with the increase in the strength of the interaction between the discrete transition and the continuous spectrum, and the corresponding reduction in F .

Figure 2 shows the calculated photoionization cross sections in the neighborhood of the giant resonance in Cr, and Mn, and the experimental data reported in Refs. 9 and 10. The latter were obtained in relative units and have therefore been normalized to the height of the main peak. On the whole, the agreement with experiment is good for both atoms. We note that our calculations took into account only one main discrete transition because the oscillator strengths for the subsequent discrete excitations were lower by two orders of magnitude. Experiment reveals a weak structure, for example, in Cr in the region of 45–48 eV (Fig. 2a), which is due to the excitation of the Rydberg series.¹⁰

It is interesting to examine the extent to which giant autoionization is reflected in the angular distribution of the photoelectrons. It is well known that this distribution is sensitive to the choice of the electron functions and to the details of the calculation and, when taken together with the partial photoionization cross sections, can be used to obtain very detailed information on the phototransition amplitudes.

With this aim in mind, we have calculated the parameter $\beta(\omega)$ (Refs. 1, 12) that characterizes the anisotropy of the angular distribution of the photoelectrons in the case of the ionization of the $3d^5$ shell of the Cr and Mn atoms. The results are shown in Fig. 3, from which it is clear that giant autoionization is also reflected in the angular distribution, producing well-defined maxima and minima on this distribution.

In conclusion of this section, we note that giant autoionization can occur only in atoms with unfilled shells. This is so, first, because the excitation of an autoionizing level occurs without a change in the principle quantum number n ($np \downarrow \rightarrow nd \downarrow$ transition) and its oscillator strength is particularly large; second, all three discrete levels corresponding to the initial, final, and intermediate states that participate in the subsequent decay also have the same n (super-Coster-Kronig transition). Hence, the decay probability and the autoionization width of the resonance are very large.

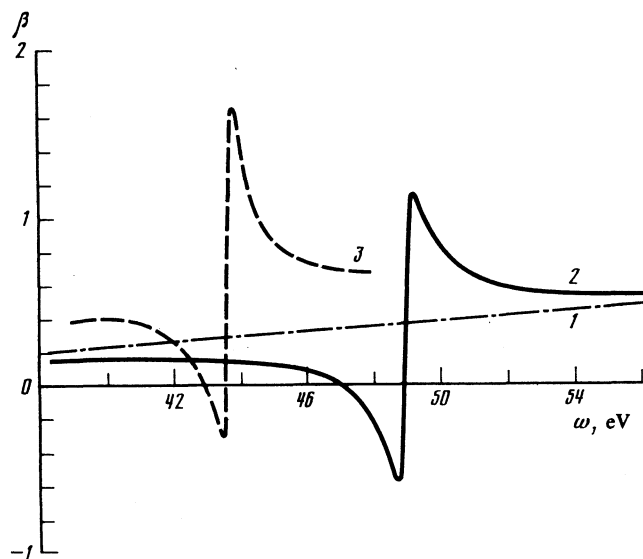


FIG. 3. Asymmetry parameter for the angular distribution of photoelectrons from the $3d^5 \uparrow$ -subshell in Mn without including the discrete $3p \downarrow \rightarrow 3d \downarrow$ transition (1) and with this transition included (2) and in Cr (3) as a function of photon energy.

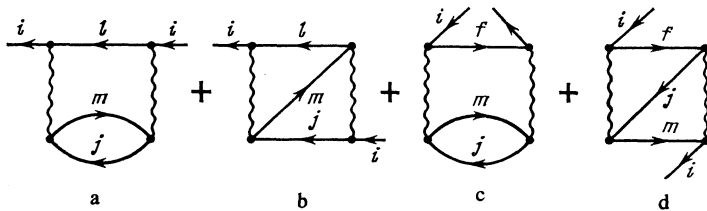


FIG. 4. Self-energy part Σ in second order in the electron-electron interaction.

4. CALCULATION OF ONE-ELECTRON LEVELS IN THE Mn ATOM

To determine the level (hole-state-energy) shifts that result from the rearrangement of the atomic core after an electron has been removed from the atom, we shall use the formalism of the self-energy part of the Green function Σ .¹ Within the framework of this formalism, the shift of the energy of the hole i is determined by the real part of the matrix element Σ_i , evaluated between the wave functions of the hole:

$$\Delta \varepsilon_i = E_i - \varepsilon_i = \text{Re} \langle i | \Sigma(E_i) | i \rangle, \quad (4.1)$$

where E_i is the Hartree-Fock value of the level energy and ε_i is the energy of the hole after the rearrangement.

We shall now confine our attention to second-order perturbation theory in the electron-electron interaction. In this approximation, the matrix elements Σ_i are determined by the diagrams shown in Fig. 4.¹ In our approach, the contribution of the exchange diagrams b and d must be excluded when the spin states of the hole i and the particle-hole pair $j-m$ are different. Correspondence rules then enable us to obtain the following analytic expression:

$$\begin{aligned} \langle i | \Sigma | i \rangle = & \sum_{j, l < F, m > F} \frac{\langle im | V | lj \rangle \langle lj | U | im \rangle}{E_i - E_l - E_j + E_m} \\ & + \sum_{m, f > F, j < F} \frac{\langle ij | V | fm \rangle \langle fm | U | ij \rangle}{E_i + E_j - E_f - E_m}, \end{aligned} \quad (4.2)$$

where the summation over $j, l < F$ is performed over all occupied states in the atom, and that over $m, f > F$ over the free states, including integration over the continuous spectrum; the matrix element $\langle ab | U | cd \rangle$ is given by (2.3). Exchange matrix elements are excluded in the case of interaction between states with different spin components μ .

The Hartree-Fock level energies¹³ in the $3d^5 \uparrow$ -, $4s^1 \uparrow$ - and $4s^1 \downarrow$ -subshells are different from the experimental values.¹⁴ Thus, the difference for the $3d^5$ - and $4s$ -shells is ~ 3 and ~ 1 eV, respectively. Calculations based on (4.2), on the

other hand, have resulted in practically complete agreement with experiment.

To determine the shift for each of the levels, we took into account the monopole, dipole, and quadrupole excitations of the atomic shells. The main contribution to the shift of the $3d \uparrow$ -level is provided by the monopole excitations of the $4s$ -shell. Its magnitude is up to ≈ 2.8 eV. The shift of the $4s^1 \uparrow$ - and $4s^1 \downarrow$ -levels is determined by the dipole excitations of the $4s \downarrow$ - and $4s \uparrow$ -electrons, respectively, and by the dipole excitations of the $3d^5$ -shell. The inclusion of only the latter, results in a shift of both $4s \uparrow$ - and $4s \downarrow$ -levels by approximately 1 eV.

The final values of the $3d^5 \uparrow$ -, $4s^1 \uparrow$ - and $4s^1 \downarrow$ -level energies, including all the above excitations of the outer shells, are listed in Table II, from which it is clear that there is good agreement with experiment.

We note that calculations of the energy shift for the deeper $3p^3 \uparrow$ - and $3p^3 \downarrow$ -shells also confirm the presence of considerable splitting of these levels.¹³ Additional up- and down-thresholds should also appear during the decay of vacancies, and one would then also observe a difference not only in the transition energies but also in the decay widths, depending on the spin of the vacancy.

5. CONCLUSIONS

We have put forward a method that can be used relatively simply and effectively to apply the formalism of the theory of the many-body problem to atoms with half-filled shells. Calculations of photoionization cross sections based on the above generalization of the RPAE approach, and the calculated level energies of the Mn atom, are in good agreement with experiment. This may be regarded as evidence for the validity of our method.

The authors are indebted to N. A. Cherepkov, S. I. Shetel', and M. Yu. Kuchiev for discussions of the foregoing topics, and to L. V. Chernysheva for the computer programs.

TABLE II. Ionization potentials for outer electrons in the Mn atom: I^{HF} —Hartree-Fock approximation, I —with allowance for many-electron correlations, I^{exp} —experimental values;¹⁴ $\Delta E^0, \Delta E^1$, and ΔE^2 —level shifts resulting from monopole, dipole, and quadrupole excitations of the subshells of the atomic core (all quantities in eV).

$n l \mu$	I^{HF}	ΔE^0	ΔE^1	ΔE^2	I	I^{exp}
$3d^5 \uparrow$	17.43	3.61	-0.15	-0.12	14.09	14.26
$4s^1 \uparrow$	7.44	0.34	-1.44	-0.05	8.59	8.61
$4s^1 \downarrow$	6.15	-0.08	-1.25	-0.03	7.51	7.43

- ¹M. Ya. Amusia and N. A. Cherepkov, *Case Stud. Atom. Phys.* **5**, 50 (1975).
- ²L. J. Armstrong, *J. Phys. B* **7**, 2320 (1974).
- ³N. A. Cherepkov and L. V. Chernysheva, *Phys. Lett. A* **60**, 103 (1977).
- ⁴J. C. Slater, *the Self-Consistent Field for Molecules and Solids*, McGraw-Hill, New York, 1974 (Russian translation, Mir, Moscow, 1978, Chap. 3).
- ⁵C. S. Fadley, D. A. Shirley, A. J. Freeman, P. S. Bagus, and J. V. Mallow, *Phys. Rev. Lett.* **23**, 1397 (1969).
- ⁶J. P. Desclaux, *Atom. Nucl. Data Tables* **12**, 311 (1973).
- ⁷J. P. Connerade, M. W. D. Mansfield, and M. A. P. Martin, *Proc. R. Soc. London, Ser. A* **350**, 405 (1976).
- ⁸R. Bruhn, B. Sonntag, and H. W. Wolf, *Phys. Lett. A* **69**, 9 (1978).
- ⁹R. Bruhn, E. Schmidt, H. Schröder, and B. Sonntag, *Phys. Lett. A* **90**, 41 (1982).
- ¹⁰R. Bruhn, E. Schmidt, H. Schröder, and B. Sonntag, Preprint DESY SR-82-08, 1982.
- ¹¹U. Fano, *Phys. Rev.* **124**, 1866 (1961).
- ¹²J. Cooper and R. N. Zare, *Lectures in Theoretical Physics*, Gordon and Breach, New York, 1969, Vol. 11 C.
- ¹³M. Ya. Amus'ya, B. K. Dolmatov, V. K. Ivanov, and S. I. Sheftel', Abstracts of Papers read to the Seventh All-Union Conf. on the Theory of Atoms and Atomic Collisions, Tbilisi, 1981, p. 11.
- ¹⁴J. M. Dyke, N. K. Fayad, A. Morris, I. R. Trickle, *et al.*, *J. Phys. B* **12**, 2985 (1979).

Translated by S. Chomet